AD-A057 702 HARRY DIAMOND LABS ADELPHI MD F/G 9/5
EMP ANALYSIS OF AN FM COMMUNICATIONS RADIO WITH A LONG-WIRE ANT--ETC(U)
JUN 78 W J STARK, G H BAKER

UNCLASSIFIED HDL-TR-1846 NL

| OF |
AD
A057702

END
DATE
FILMED
9-78
DDC

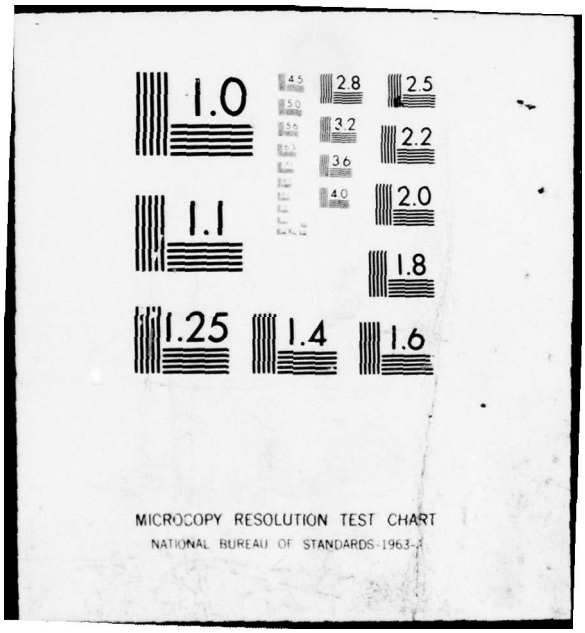
1.0
1.1
1.25
1.4
1.6
1.8
2.0
2.2
2.5
2.8
3.2
3.6
4.0
4.5
5.0
5.6
MICROCOPY RESOLUTION TEST CHART
NATIONAL BUREAU OF STANDARDS-1963-A

HDL-TR-1846

June 1978

EMP Analysis of an FM Communications Radio with a Long-Wire Antenna

by Werner J. Stark and George H. Baker

U.S. Army Electronics Re
and Development Com
Harry Diamond Labora
Adelphi, MD

The findings in this report are not to be construed as an official Department of the Army position unless so designated by other authorized documents.

Citation of manufacturers' or trade names does not constitute an official indorsement or approval of the use thereof.

Destroy this report when it is no longer needed. Do not return it to the originator.

DEPARTMENT OF THE ARMY
Harry Diamond Laboratories
2800 Powder Mill Rd
Adelphi, MD 20783

UNCLASSIFIED

SECURITY CLASSIFICATION OF THIS PAGE *(When Data Entered)*

REPORT DOCUMENTATION PAGE

READ INSTRUCTIONS BEFORE COMPLETING FORM

(14) 1. REPORT NUMBER: HDL-TR-1846

2. GOVT ACCESSION NO.

3. RECIPIENT'S CATALOG NUMBER

(6) 4. TITLE *(and Subtitle)*: EMP Analysis of an FM Communications Radio with a Long-Wire Antenna

(9) 5. TYPE OF REPORT & PERIOD COVERED: Technical Report

6. PERFORMING ORG. REPORT NUMBER

(10) 7. AUTHOR(s): Werner J. Stark and George H. Baker

8. CONTRACT OR GRANT NUMBER(s)

9. PERFORMING ORGANIZATION NAME AND ADDRESS
Harry Diamond Laboratories
2800 Powder Mill Road
Adelphi, MD 20783

10. PROGRAM ELEMENT, PROJECT, TASK AREA & WORK UNIT NUMBERS
DA: 1W162118AH75/A-29
DNA: R99QAXEB075/61

11. CONTROLLING OFFICE NAME AND ADDRESS
U.S. Army Materiel Development and Readiness Command
Alexandria, VA 22333

and

Director
Defense Nuclear Agency
Washington, D.C. 20305

(11) 12. REPORT DATE: June 1978

13. NUMBER OF PAGES: 37

(12) 33 p.

15. SECURITY CLASS. *(of this report)*: Unclassified

15a. DECLASSIFICATION/DOWNGRADING SCHEDULE

16. DISTRIBUTION STATEMENT *(of this Report)*

Approved for public release; distribution unlimited.

(11) B075, A29

17. DISTRIBUTION STATEMENT *(of the abstract entered in Block 20, if different from Report)*

(16) 1W162118AH75, R99QAXE

18. SUPPLEMENTARY NOTES: This work was sponsored by the Department of the Army under Project 1W162118AH75/A-29, Multiple Systems Evaluation Program, and by the Defense Nuclear Agency under Subtask R99QAXEB075, Work Unit 61, Ground-Based Antenna Systems' (cont'd on back)

19. KEY WORDS *(Continue on reverse side if necessary and identify by block number)*

Computer network analysis
AN/PRC-77
EMP effects analysis
Antenna network synthesis
Long-wire antenna
HF antenna
Antenna impedance
Antenna effective height
Antenna equivalent circuit

20. ABSTRACT *(Continue on reverse side if necessary and identify by block number)*

A Norton equivalent circuit is developed for a long-wire antenna used with a man-pack FM radio exposed to an incident electromagnetic pulse (EMP). The required short-circuit current and antenna impedance are computed by use of a transmission-line model for the antenna, and the computations are compared with measurements of the short-circuit current and antenna impedance. The comparison shows that the transmission-line model for the antenna is adequate for performing a vulnerability analysis of the radio. (cont'd on back)

DD FORM 1 JAN 73 1473 EDITION OF 1 NOV 65 IS OBSOLETE

UNCLASSIFIED

1 SECURITY CLASSIFICATION OF THIS PAGE *(When Data Entered)*

Y63 050

(18) Characterizations

HDL project: X756E2 PRON: A1-6-R0004-01-A1-A9
DRCMS code: 612118.H750011 Program element: 62118A

DNA project: E196E3 MIPR: 6.00511
DRCMS code: 697000.22.11443.WJ-A1 Program element: 62704A

(20) A network model is developed for a portion of the radio and is used as the load in the Norton equivalent circuit. Load currents in response to an incident electromagnetic pulse from the Army EMP Simulator Operation (AESOP) are computed when the radio is tuned to specific frequencies in the low and high bands. The computed load currents are compared with experiment and show excellent agreement between theory and experiment.

CONTENTS

FIGURES

FIGURES (Cont'd)

1. INTRODUCTION

1.1 Description of Radio and Antenna

The AN/PRC-77 radio set is a frequency-modulated (FM) receiver transmitter used to provide two-way voice communication. This short-range manpack-portable radio set is fully transistorized and can be operated over two bands covering the frequency range from 30 to 75.95 MHz. The radio set can be used with a number of different types of antennas such as monopole, dipole and log-periodic. In this paper we will analyze the radio when it is used with a long-wire antenna, as shown in figure 1. The antenna is simply a thin wire 45.72 m long, supported parallel to ground at a height of approximately 1.22 m above ground. When placed in this manner, the radio is used for communications in the direction of the wire antenna with an angular range of approximately 12 deg on either side of the antenna.[1]

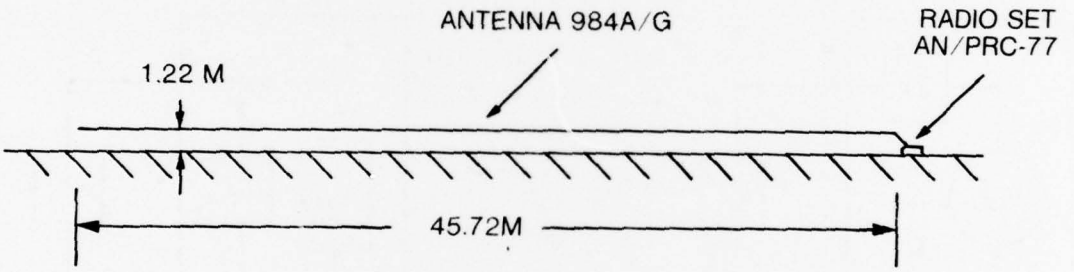

Figure 1. Radio set AN/PRC-77 used with antenna AT-984A/G.

1.2 Analysis Approach

Since the receiver contains nonlinear components, we must analyze the antenna with nonlinear loads. A useful approach to this problem for dipole and monopole antennas has been developed by Toulios,[2] who uses a lumped-parameter network (LPN) representation of both the effective height and the antenna impedance. With this approach, the antenna is represented in terms of a Thevenin equivalent

---

[1] *Department of the Army, Operator's and Organizational Maintenance Manual, Including Repair Parts List: Radio Set AN/PRC-77, TM 11-5820-667-12 (June 1967).*

[2] *P. P. Toulios, Antenna User's Manual for Cylindrical Antennas, Vol I, Illinois Institute of Technology Research Institute (January 1974).*

circuit in which the source voltage is generated by the transient voltage representing the incident electromagnetic pulse (EMP) operating on the effective height circuit. When the dipole or monopole antenna is located near ground, the source voltage also operates on a network which takes into account the ground interaction. Once the Thevenin equivalent circuit has been defined it can be included with the network representing the antenna load, and standard network analysis techniques can be used to determine the energy delivered to the various circuit components, including nonlinear devices.

Figure 2 shows that the above technique can be simplified somewhat by representing the antenna with either a Thevenin or Norton equivalent circuit, in which the source (open-circuit voltage or short-circuit current) is computed directly from antenna theory, rather than from network analysis of the effective height circuit. Since the network analysis of the Thevenin or Norton equivalent circuit is performed in the time domain, the antenna impedance for this circuit must be represented in terms of its equivalent LPN.

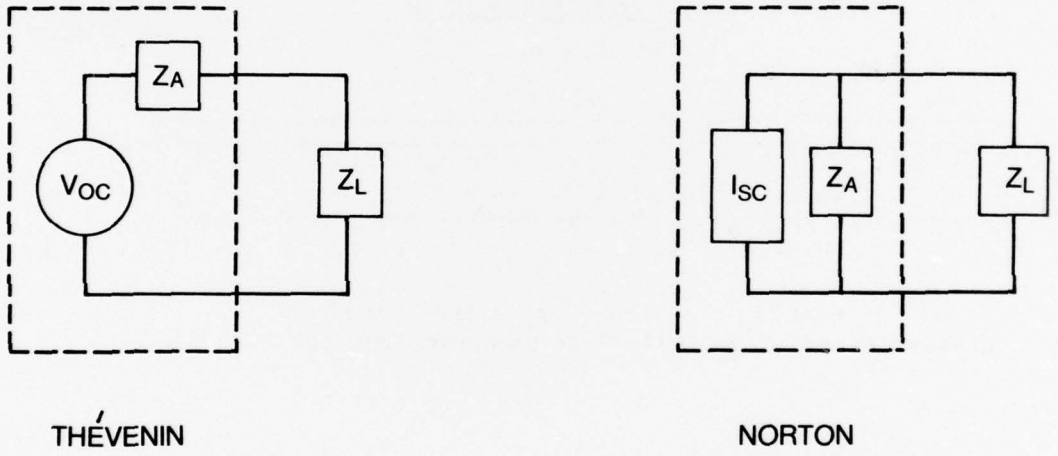

Figure 2. Equivalent circuits for an antenna.

2. EQUIVALENT CIRCUIT FOR ANTENNA

2.1 Antenna Impedance

The antenna is approximately 50 m long; thus, multiple resonances will be excited when it is driven by the frequency spectral content of an incident electromagnetic pulse (EMP). Under these conditions the antenna certainly cannot be considered to be effectively

small; i.e., we cannot simply represent the antenna impedance by a single capacitor or inductor. Our approach toward determining the network representation of the antenna impedance will be to compute this impedance in the frequency domain from an approximate analytical model valid over the appropriate frequency range and then to apply network synthesis to determine the LPN for this impedance.

We can model the antenna in terms of a single conductor parallel to a finitely conducting ground, terminated by a load at one end and open at the other end. An approximate solution for this geometry can be obtained in terms of a transmission-line model,[3] in which the transmission line consists of the conductor and its image in the ground plane. This approximate solution has been applied to specific EMP transient problems[4] and is described in the DNA-2114 EMP Handbook.[5] Figure 3 (p 8) shows a comparison of the solution for the antenna impedance (computed from the transmission-line model) with experimental data for the antenna impedance. The measurements were made by driving the antenna from an external source and measuring the ratio of induced voltage to current over the frequency range of interest. Described elsewhere[6] are details of the measurement process using the Harry Diamond Laboratories continuous wave facility (HDL-CW).

2.2 Network Synthesis for Antenna Impedance

The subject of network synthesis is discussed in detail in many textbooks. A necessary and sufficient condition for an impedance function to be realizable as an LPN is that the function be positive real.[7] This condition is satisfied by the antenna impedance for the long-wire antenna. We can determine the LPN for this impedance by making the observation that behavior of the impedance function at each of the resonances is similar to that of the impedance of a parallel resonant circuit. The R, L, and C values of this circuit can be determined from the amplitude, location, and Q of the resonance. The total LPN for the antenna impedance is then obtained from the series sum of the LPN's of all the parallel resonant circuits for all the

---

[3] *E. D. Sunde, Earth Conduction Effects in Transmission Systems, Dover Publications, Inc., New York (1968).*

[4] *W. E. Scharfman, K. A. Graf, and E. F. Vance, Analysis of Coupling to Horizontal and Vertical Wires, Stanford Research Institute, SRI Technical Memorandum No. 22 (1972).*

[5] *E. F. Vance, Defense Nuclear Agency-2114 EMP Handbook, Ch 11, Coupling to Cables (December 1974).*

[6] *W. J. Stark, Transient Response of a Log-Periodic Antenna Based on Broadband CW Measurements, Harry Diamond Laboratories TR-1792 (April 1977).*

[7] *E. A. Guillemin, Synthesis of Passive Networks, John Wiley & Sons, Inc., New York (1957).*

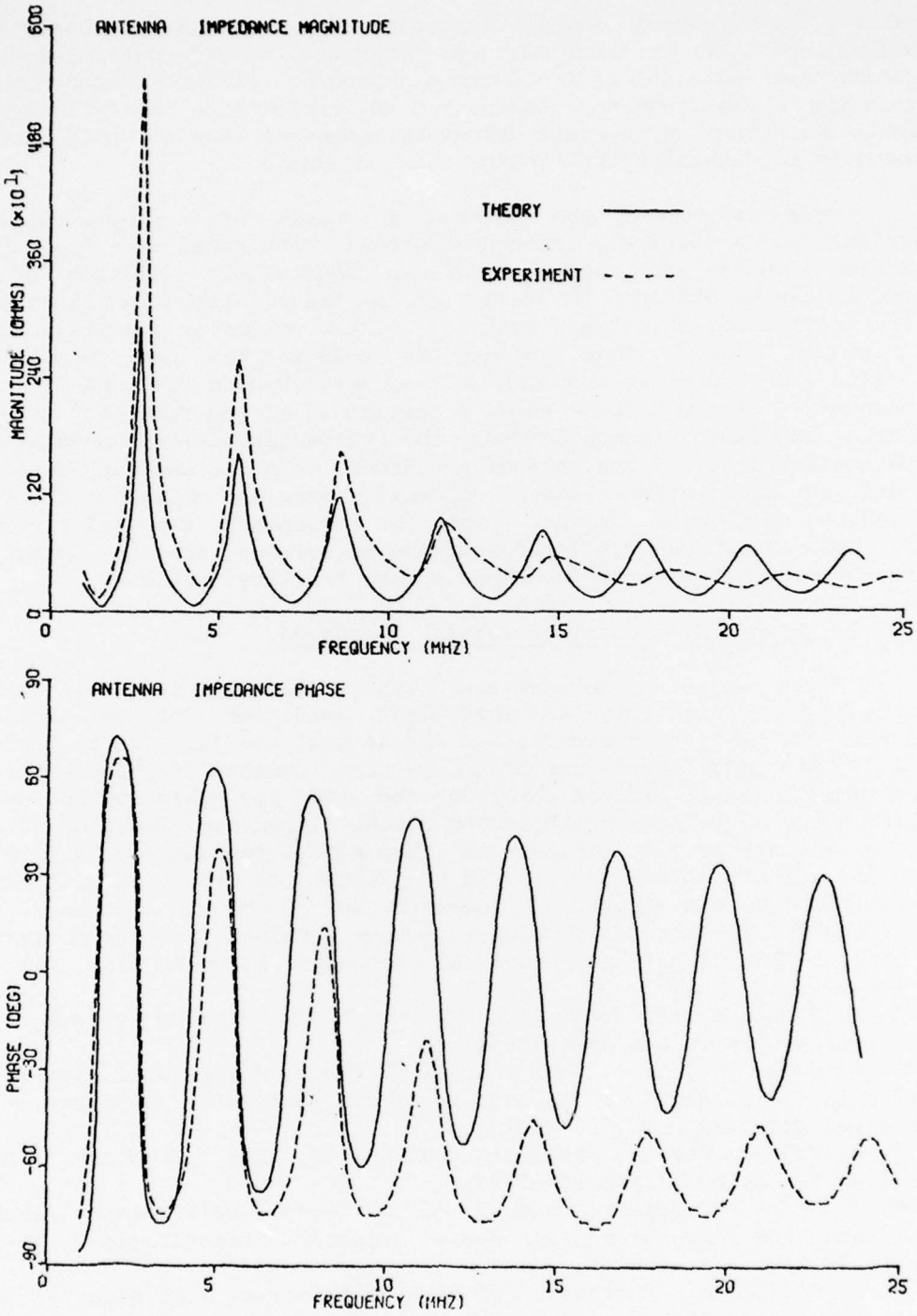

Figure 3. Comparison of theory and experiment for antenna impedance.

resonances over the frequency range of interest. This technique applies also to network synthesis of input impedance for multiconductor transmission lines, and excellent comparisons can be obtained for impedance functions and corresponding synthesized networks.[8] For the long-wire antenna, the impedance shows approximately a $1/\omega$ dependence between zero frequency and the location of the first antiresonance. This behavior can be adequately described by a capacitor in series with the parallel resonant circuits. The synthesized network for the antenna impedance is then as shown in figure 4.

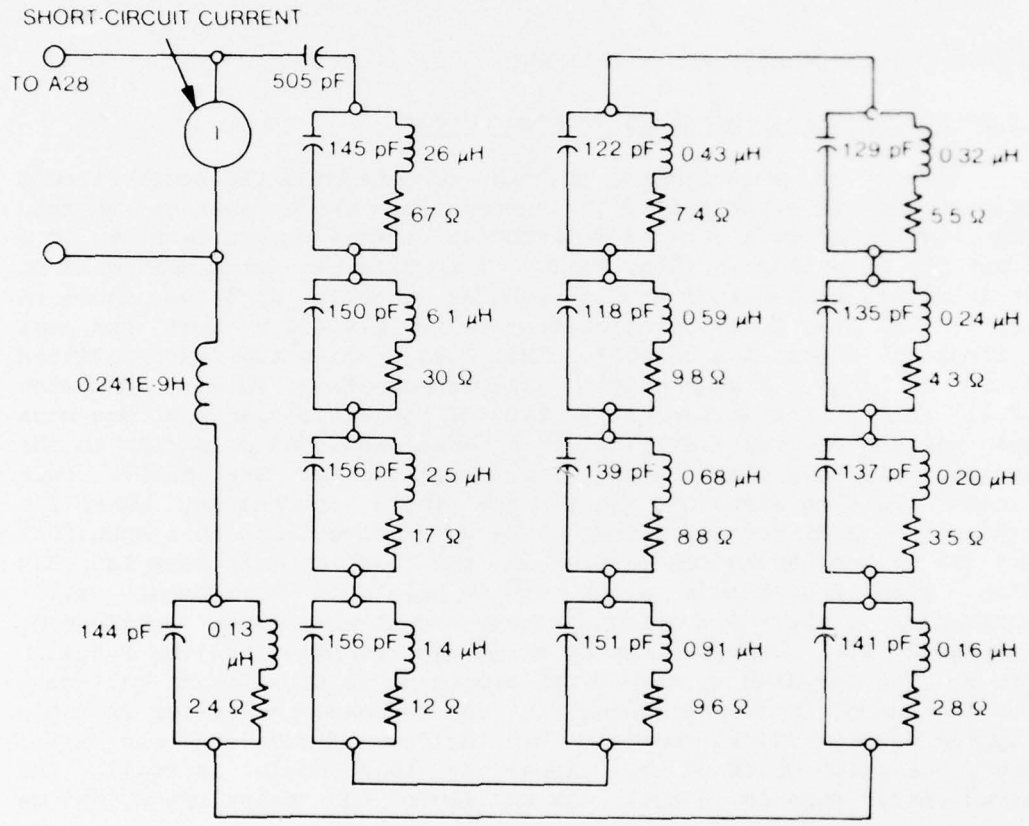

Figure 4. Equivalent circuit for long-wire antenna.

---

[8] *Janis Klebers, User's Manual for the NLINE Multiconductor Transmission-Line Computer Code, Harry Diamond Laboratories TR-1803 (May 1977).*

2.3 Equivalent Short-Circuit Current

For the present analysis we will choose the Norton equivalent circuit for the antenna, so we must compute the antenna's short-circuit current. Our model of the antenna is that of a single conductor parallel to a finitely conducting ground. An approximate solution for this model is given in the DNA-2114 EMP Handbook (eq. 11.4-53)[5] for arbitrary angles of incidence relative to the ground plane and the conductor. Since the solution is only approximate, we will first evaluate the solution by comparison with experimental data. If we are satisfied with the accuracy of the solution, we will then determine the worst-case angle of incidence of the EMP.

3. COMPARISON OF THEORY AND EXPERIMENT

3.1 Horizontally Polarized Incident Field

A set of measurements was made to determine the short-circuit current at the receiver end of the antenna when the antenna was shorted to the case of the receiver and oriented at various angles relative to a horizontally polarized incident field. The receiver was positioned on earth (finitely conducting) ground with the antenna used as shown in figure 1. The system was positioned approximately 450 m from the Army EMP Simulator Operation (AESOP). This simulator is the fixed-position version of the Transportable Electromagnetic Pulse Simulator (TEMPS).[9] Since the horizontal section of the radio's antenna was much longer than the vertical section, the antenna responded primarily to the horizontal electric field along its length. For the AESOP, this horizontal field consists of radial and theta components, where the radial and theta directions refer to the usual directions in a spherical coordinate system having its origin in the gap of the wave-launcher section with the Z-axis along the simulator's horizontal axis. Measurements of the radio antenna's response to the AESOP environment are compared with computations by using the transmission-line model in figure 5. The response to the radial component is significant only near end-on incidence. Peak amplitudes in the response result for an angle of approximately 23 deg between the incident field and the wire; however, the pulse width of the signal at this angle is small. The received energy depends on both peak amplitude and pulse width, and we

---

[5] *E. F. Vance, Defense Nuclear Agency EMP Handbook, 2114, Ch 11, Coupling to Cables (December 1974).*

[9] *Eugene L. Patrick and Spencer L. SooHoo, Transportable Electromagnetic Pulse Simulator (TEMPS) Field Mapping Report, Harry Diamond Laboratories TR-1743 (September 1976).*

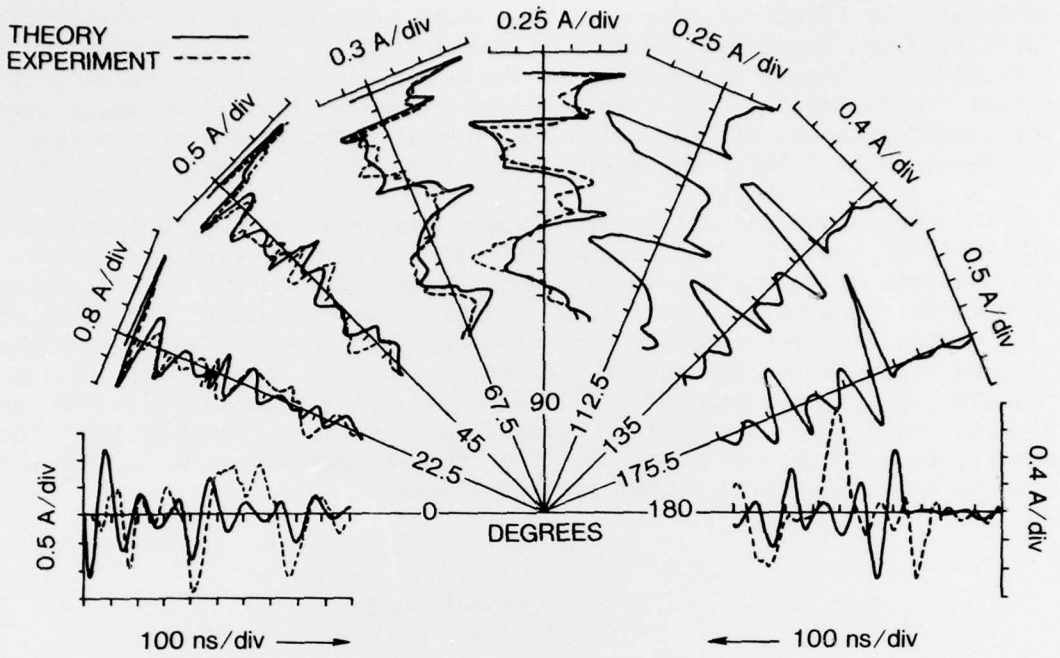

Figure 5. Computed and experimental short-circuit current on antenna for various angles of incidence of transient field from AESOP.

will see in a later section that for this particular antenna, the worst-case angle of incidence is not necessarily the angle resulting in maximum amplitudes of the received signal.

3.2 Vertically Polarized Field

The short-circuit current at the receiver end of the antenna was also measured when the antenna was illuminated by a transient pulse from a 30-m vertical monopole antenna. Measurements were made for both end-on and broadside incidence. We will show only the results for end-on incidence, since, as we would expect, the response for end-on incidence was significantly higher than for broadside. For end-on incidence, the receiver was 90 m from the transmit antenna, with the long-wire antenna pointing directly at the transmit antenna. Both the vertical and radial components of the incident field were measured in the absence of the receive antenna at 30, 60, and 90 m from the transmit antenna. The overall waveshapes of the measured fields varied only slightly for both components, except that they both exhibited a 1/R dependence, and the high-frequency components were more rapidly

attenuated at large distances. The radial component of the electric field results from the fact that the vertically polarized wave has a forward tilt[10] near the surface of the earth, due to the earth's finite ground conductivity. Our measurements showed that the waveshape for both components was similar, with the overall amplitude of the radial component about 1/10 of the amplitude of the vertical component.

The upper part of figure 6 shows measured vertical component of the incident electric field component 60 m from the transmit antenna. The analytic approximation was obtained from a fit to the data by using exponential functions. The radial electric field component was taken as 1/10 of the vertical component and was used in the computations of the antenna response for the end-on incidence. The 1/R dependence of the radiated field was ignored for this computation; instead, we used an average value of the field. The results of the measurements and the analytical predictions based on the transmission-line model for the antenna are shown in the lower part of figure 6.

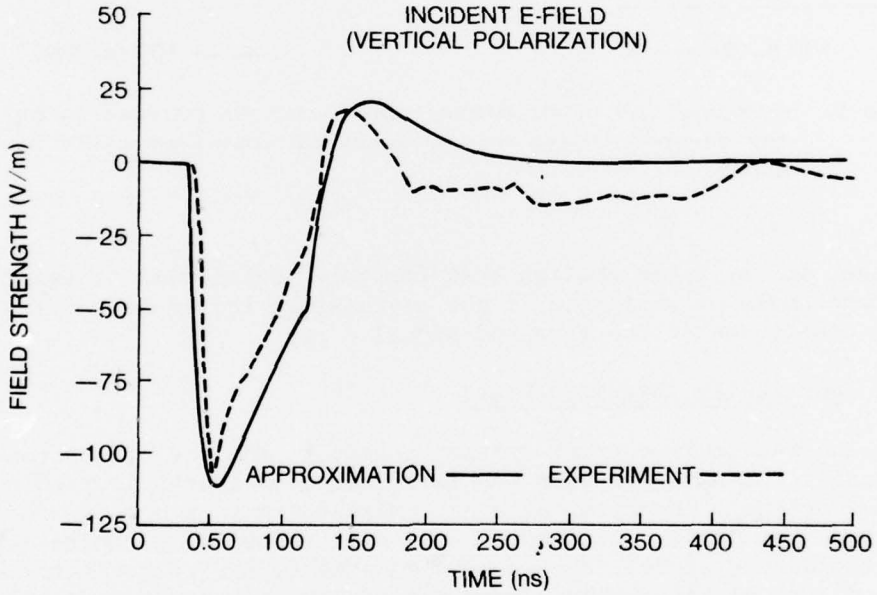

Figure 6. Computed and experimental short-circuit current on antenna for end-on incidence of transient field from a vertical monopole antenna (cont'd on p 13).

[10] *E. C. Jordan and K. G. Balmain, Electromagnetic Waves and Radiating Systems, Prentice-Hall, Inc., Englewood Cliffs, NJ (1968).*

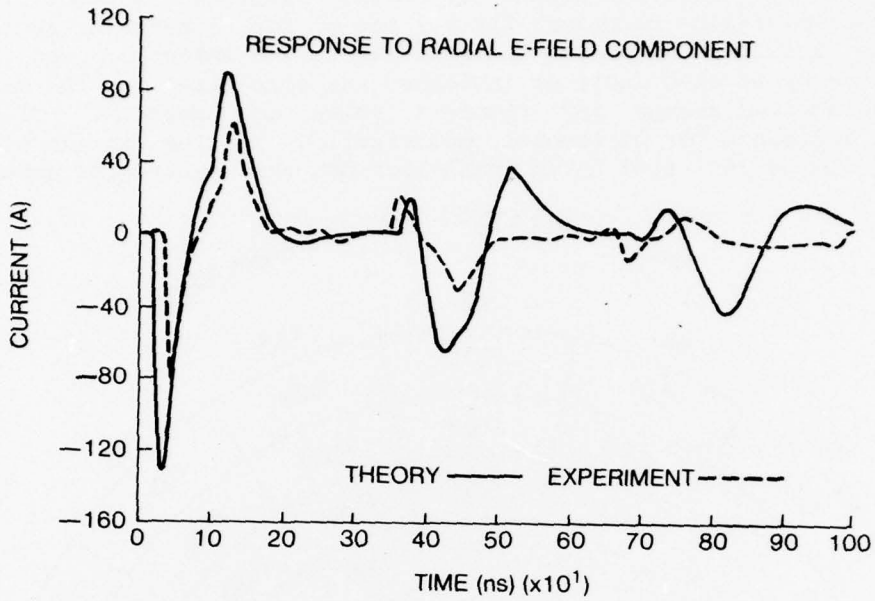

Figure 6. Computed and experimental short-circuit current on antenna for end-on incidence of transient field from a vertical monopole antenna (cont'd from p 12).

4. WORST-CASE ORIENTATION OF ANTENNA

4.1 Maximum Energy Received by Antenna

The purpose of studying the EMP response of an antenna is to utimately compute the energy delivered to a receiver connected to the antenna, so that one can determine any possible vulnerability of the receiver components. Before computing the maximum energy delivered to the receiver, we will compute the maximum possible energy received by an ideal load. From the maximum-power transfer theorem, such a load is equal to the complex conjugate of the antenna impedance.

A corollary to the maximum-power transfer theorem states that the maximum power which can be absorbed from a source network equals $V_{oc}^2/4\ \mathrm{Re}\ (Z_s)$, where V_{oc} is the open-circuit voltage at the source and $\mathrm{Re}\ (Z_s)$ is the real component of the source impedance. If we use this corollary, the maximum energy, E, received by an antenna terminated in the complex conjugate of the antenna impedance is equal to

$$E = 1/2 \int_0^\infty \frac{|V_{oc}|^2}{\mathrm{Re}(Z_A)}\ df \quad .$$

We computed the above expression for E using numerical integration and the transmission-line solutions for V_{oc} and Z_A for a range of angles of incidence relative to ground and relative to the antenna. The total maximum energy at each angle of incidence was normalized to the maximum possible received energy and figure 7 shows the results. Clearly, overhead incidence for horizontal polarization results in the maximum possible energy delivered to an ideal load for this particular antenna.

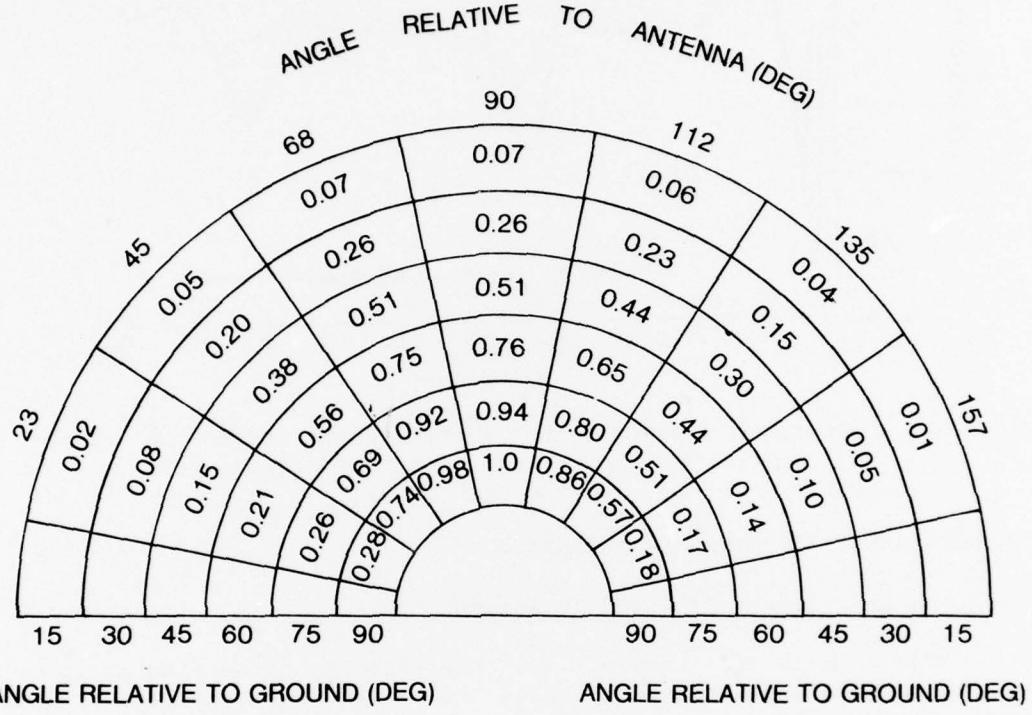

Figure 7. Relative maximum energy received by antenna for various angles of incidence of high-altitude EMP.

4.2 Maximum Energy Input to Receiver

The fundamental resonant frequency of our long-wire antenna is approximately 3 MHz, whereas the receiver can be tuned to a frequency range of 30 to 76 MHz. Obviously, the load represented by the receiver cannot possibly receive the maximum energy received by the ideal load described in the previous section. In order to estimate the energy received when the receiver is tuned to a given frequency, we must examine V_{oc} over the entire operating frequency range for various angles of the incident EMP relative to ground and the antenna. The results for such a parametric study are shown in figure 8, and we can make some

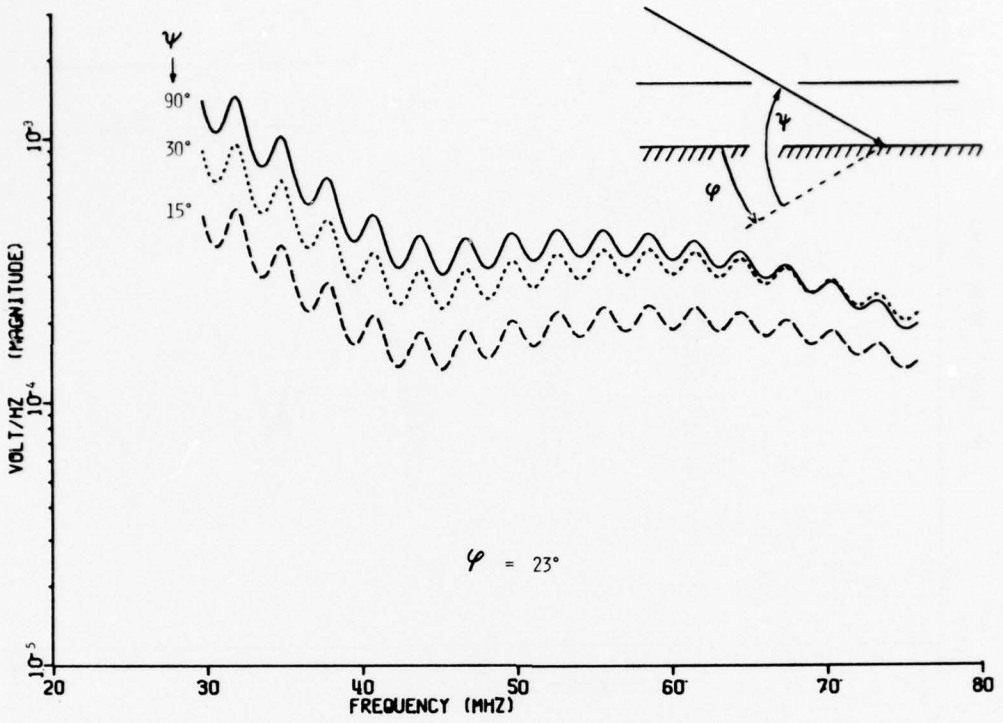

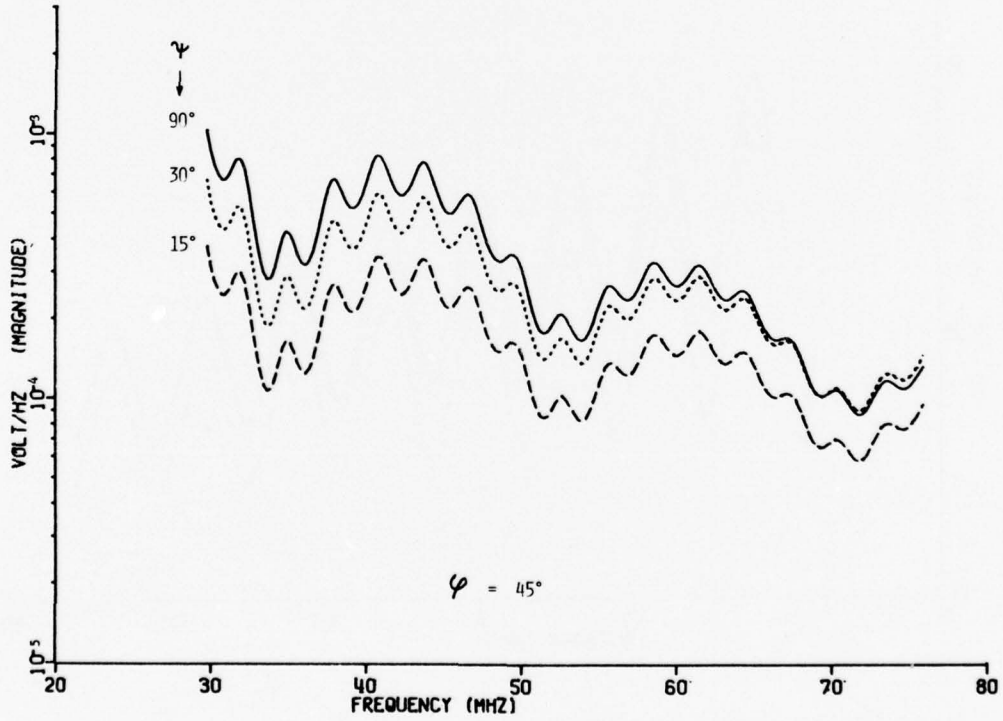

Figure 8. Open-circuit voltage over operating bands of radio; (a) γ = 23 and 45 deg (cont'd on p 16).

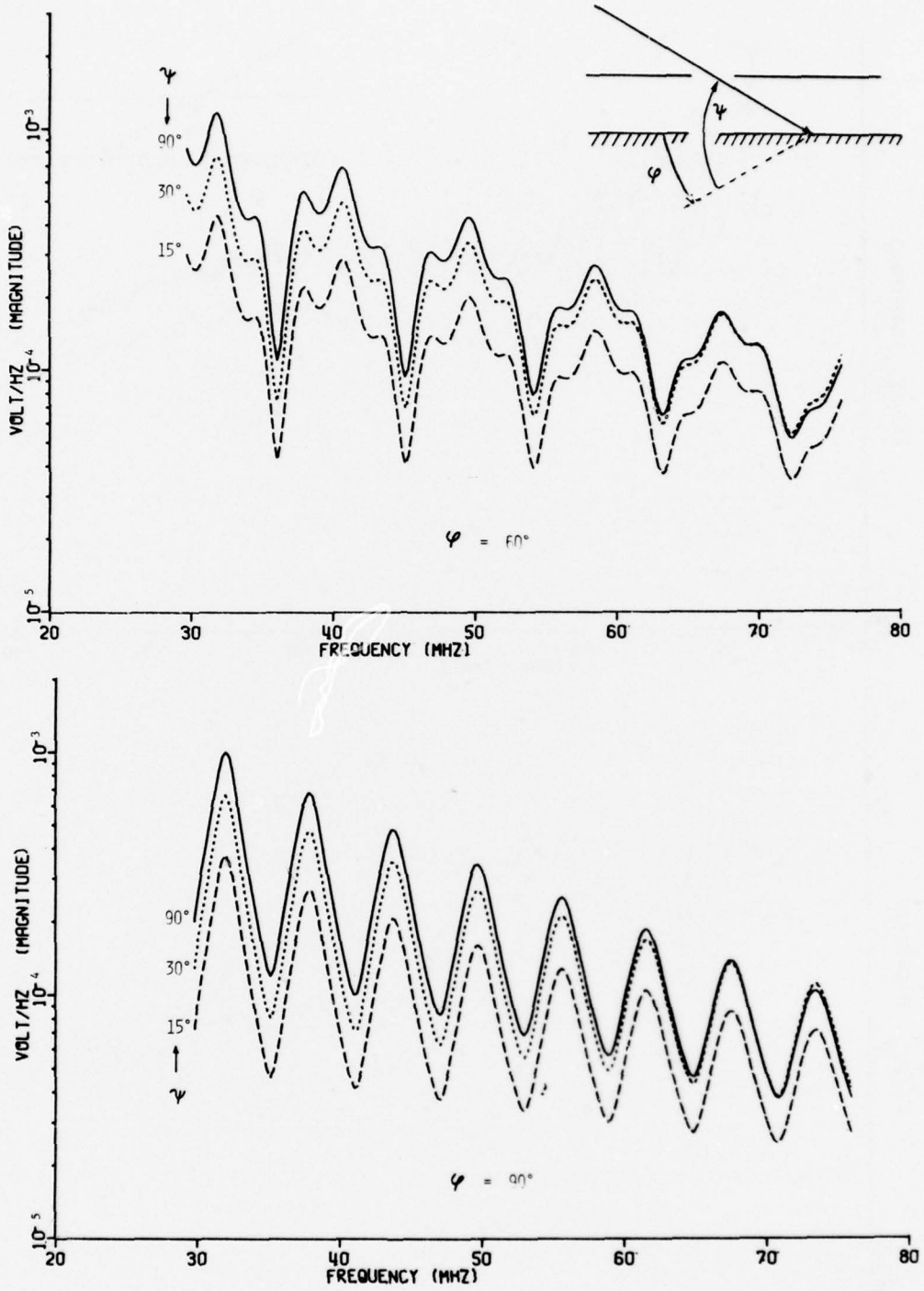

Figure 8. Open-circuit voltage over operating bands of radio; (b) γ = 60 and 90 deg (cont'd from p 15).

general observations from these results. For almost all frequencies, and for all angles of incidence relative to the wire, peak V_{oc} results for overhead incidence at the lower end of the operating frequency range. When the receiver is tuned to the low band, the input impedance to the receiver is essentially zero, except for a narrow band of frequencies approximately 1 MHz wide centered about the tuning frequency. Thus, all frequency components are filtered by the tuning network, except those near the tuning frequency. The total energy that can be transmitted to sensitive receiver components is given from equation (1), where the integration is carried out only over the 1-MHz bandwidth at the tuning frequency. At frequencies above 30 MHz, Re (Z_A) varies slowly as a function of frequency, so the variation in received energy essentially depends on the integral of $|V_{oc}|^2$ over the tuning range. It is clear from figure 8 that maximum energy is transmitted to sensitive receiver components from overhead incidence when the receiver is tuned to approximately 31.5 MHz, with a worst-case angle of incidence of 23 deg relative to the antenna. Although some geometry could result in a higher energy transfer, we can see that the maximum energy at 31.5 MHz for overhead incidence does not vary to a great extent for the various angles relative to the antenna. Thus, we might expect that energy computations using a finer grid for various angles of incidence will not result in energy estimates much larger than that for overhead incidence at 23 deg.

5. NETWORK ANALYSIS OF THE RADIO

5.1 Network Model for the Radio

The AN/PRC-77 radio set is described fully in the maintenance manual[11] for the radio. Figure 9 shows a block diagram for the radio set as used with the various optional antennas. In this paper we will investigate the coupling of the long-wire antenna at the short/long antenna terminal into module A28 through module A32 to the transmitter power amplifier (module A36).

Amplifier A36 is a 2-W class-C, common-emitter, transistor power amplifier with single-tuned input and output circuits. A switch controls the tuning circuits for high-band (53.00-75.95 MHz) or low-band (30.00-53.00 MHz) operation. Figure 10 shows the low-band circuit topology. For low-band operation, transformer T1 and capacitors C1, C2, and C1B comprise the tuned circuit. Variable gang capacitor C1B provides continuous tuning across the band. Transformer T3 and capacitors C8, C9, and gang capacitor C1A comprise the tuned circuit.

---

[11] *Department of the Army, DS, GS and Depot Maintenance Manual: Radio Set AN/PRC-77, TM 11-5820-667-35 (16 February 1968).*

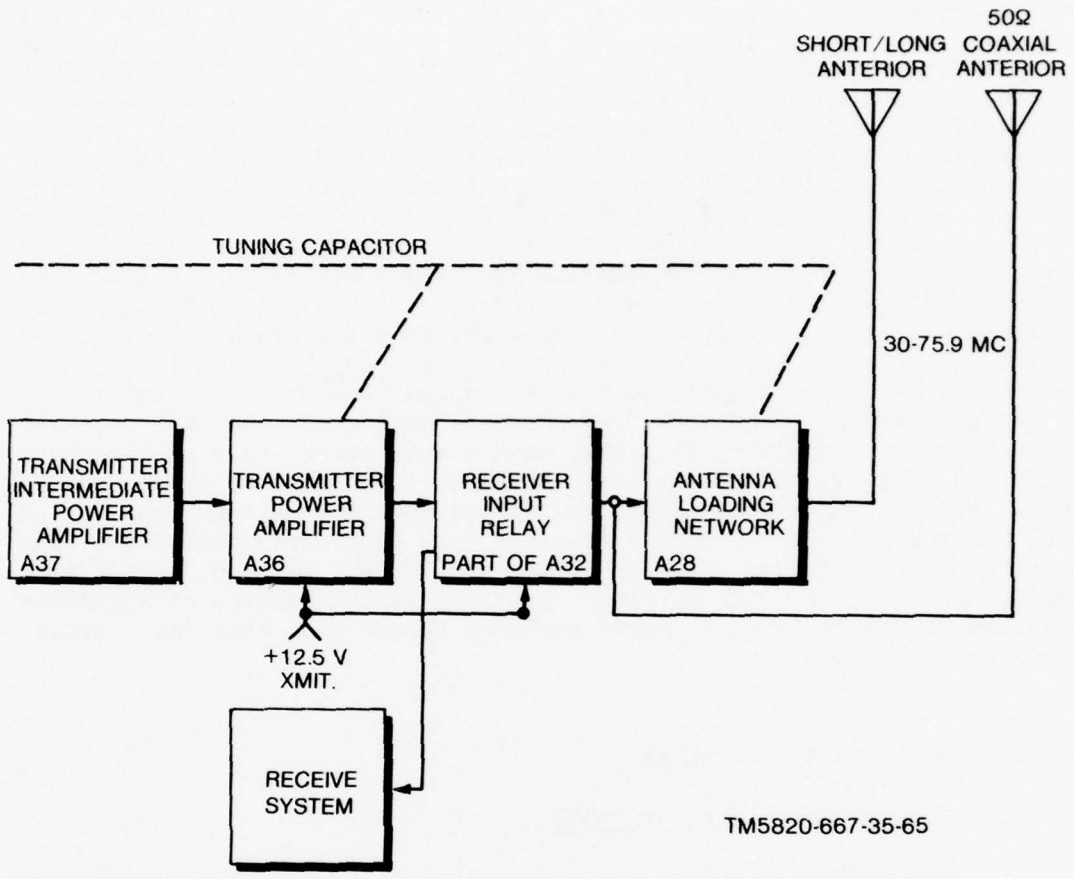

Figure 9. Block diagram for AN/PRC-77 radio set (excerpted from Department of Army TM 11-5820-667-35).

Inductor L5 matches the load impedance to the collector of transistor Q1. Inductor L6 and capacitor C10 form a low-pass rf filter to suppress harmonic radiation. The parallel combination of resistors R10 and R11 provides a load to the collector Q1.

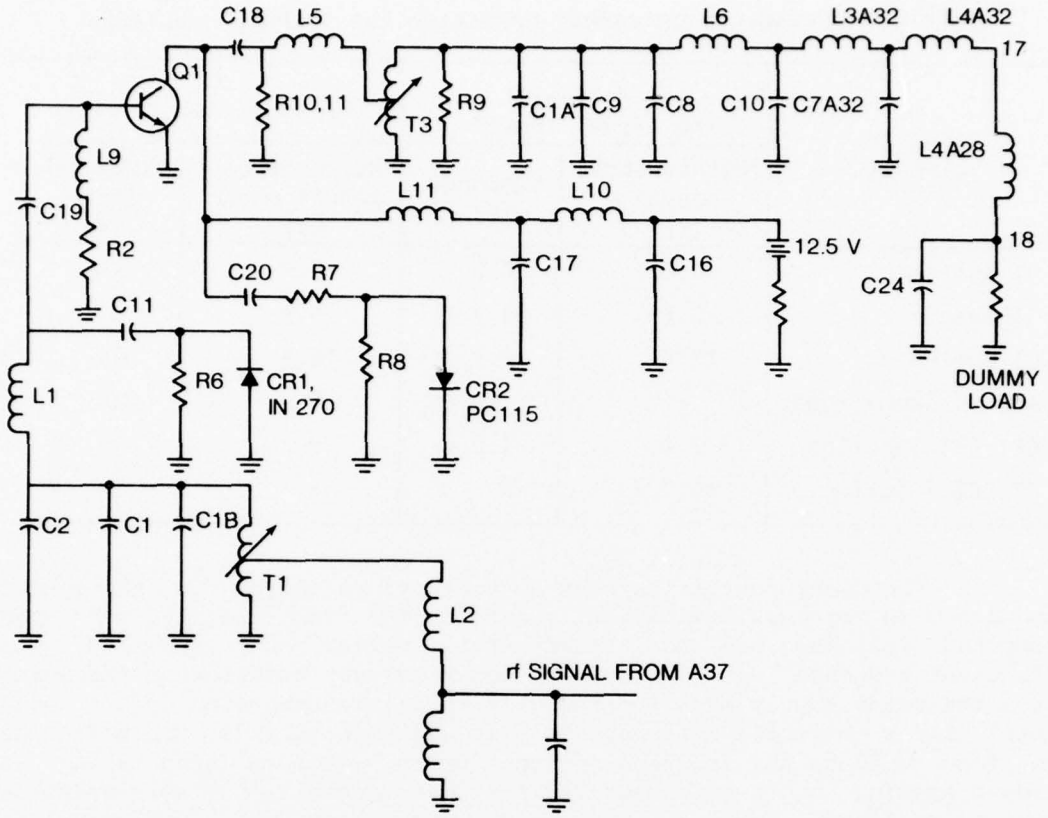

Figure 10. Low-band circuit topology for radio set AN/PRC-77 in transmit mode (modules A28, A32, and A36).

5.2 Validation of Radio Network Model

The depot maintenance manual describes a signal trace performed by inserting a 130-ohm dummy load at the output of A28 and applying a 6 V, 30-MHz rms signal to the input of A36. The manual then specifies the resulting dc and signal levels at key points within the module.[11] A computer run was made for the network shown in figure 10 and table I shows a comparison of computed results and values specified in the maintenance manual for selected points in the circuit. Table I(a) shows the dc levels for no signal input and Table I(b) shows the rms levels when the 6-V rms signal is applied to the input of module A36.

---

[11] *Department of the Army, DS, GS and Depot Maintenance Manual: Radio Set AN/PRC-77, TM 11-5820-667-35 (16 February 1968).*

TABLE I. COMPARISON OF MANUAL-SPECIFIED AND COMPUTED VOLTAGES

Point in circuit	(a) dc levels (no signal input)		(b) ac signal levels	
	Maintenance manual (V)	Computed (V)	Maintenance manual (rms) (V)	Computed (rms) (V)
Q1 emitter	0.0	0.0	0.0	0.0
Q1 base	0.89	0.7	3.9	2.5
Q1 collector	12.5	12.2	16.5	16
Across dummy load	-	-	6	10
C11-CR1 junction	2.2	1.0	-	-
R7-CR2 junction	-5.5	-8	-	-

The discrepancies between ac voltages specified in the manual and computed voltages are partially due to the fact that the tabulated computed voltages are not steady-state values but represent the transient response out to 1 μs. Low-frequency transients introduced from the power supply when the radio is initially turned on do not decay until after several microseconds. In addition to this, the model was not fine tuned to the frequency of the driving waveform (such tuning is time-consuming on the computer) so that optimized network response was not realized. However, the above comparison was good enough to indicate that the simulated circuit was functional and reasonably close in operating level to the actual circuit. The power dissipated in the semiconductors during normal operation was noted for comparison with that dissipated during an EMP excitation.

5.3 Received Transient Signals--Comparison of Theory and Experiment

When the antenna was driven by transient fields from the AESOP, the Thevenin equivalent circuit for the antenna (fig. 4) was combined with the network model for the radio (fig. 9) and the transient response of the system was computed. Figure 11 shows the comparison of the computed and measured current at the input to the radio with the radio tuned to 30 MHz on the low band. Figure 12 shows the same type of comparison with the receiver tuned to 75 MHz on the high band. The agreement is excellant in view of all the errors in both the network analysis and the experiment.

Having validated the theoretical model for the antenna response, the radio network model, and the combination of the two models, the EMP response of the radio could be computed. The results of

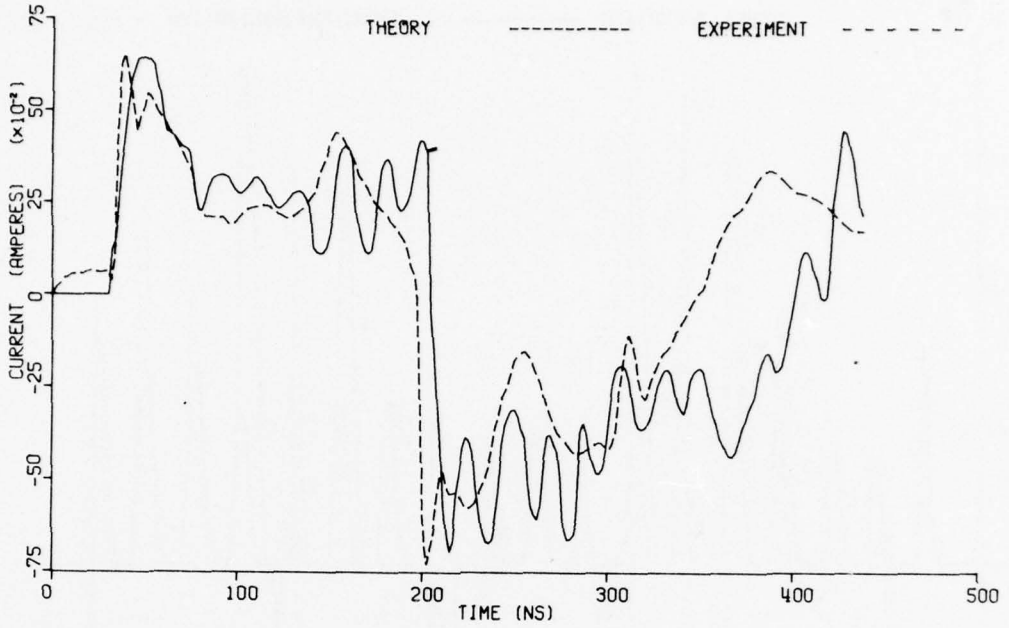

Figure 11. Transient current at input to radio (low band).

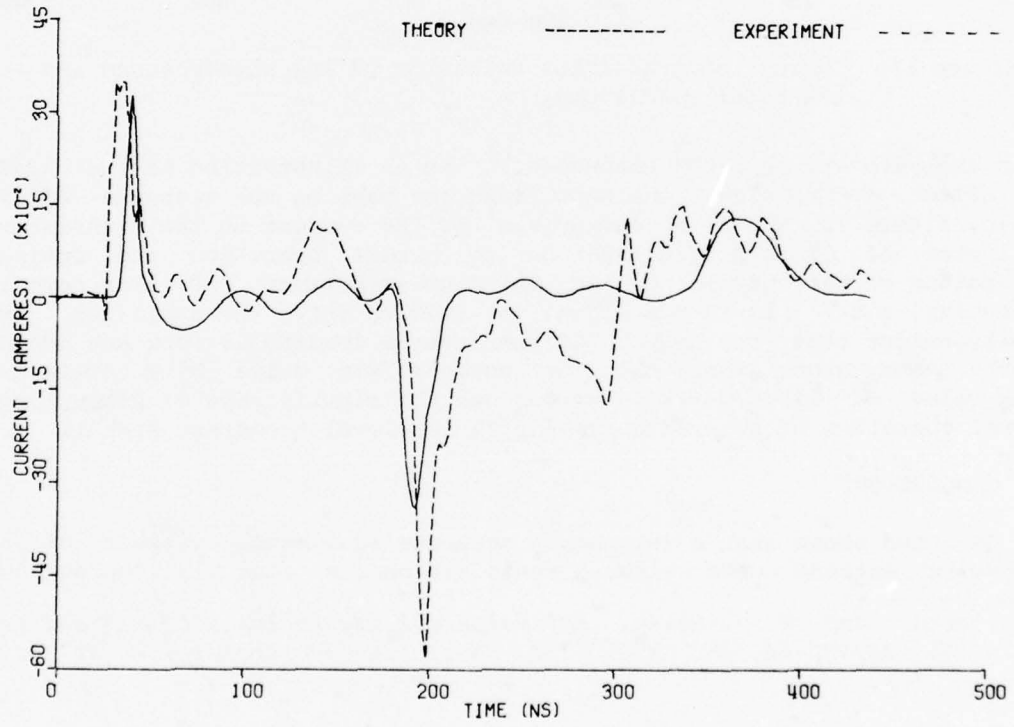

Figure 12. Transient current at input to radio (high band).

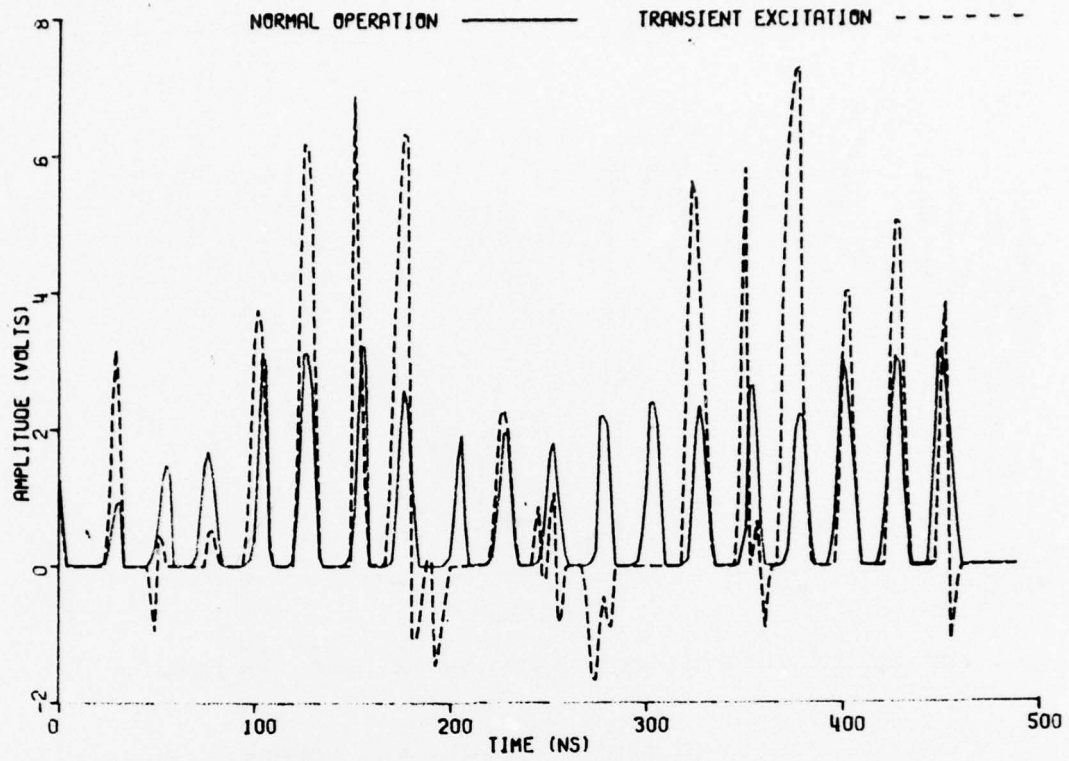

Figure 13. Current on transistor collector Q1 for steady-state and transient conditions.

this analysis are reported elsewhere.[12] As an illustration of the kind of effect a transient incident field can have on the response of a radio, figure 13 shows a comparison of the current on the transistor collector of Q1 (amplifier A36) during normal operation and during excitation of the antenna by an incident transient EMP. For normal operation, a 6-V rms 30-MHz signal was used to drive the amplifier. In the transient case, the output of the antenna loading network was added to the steady-state signal when the antenna was driven by a low-level peak value of 218-V/m EMP. We can see the significance of disrupting normal operation of the radio, even by a low-level transient signal.

6. CONCLUSIONS

We have shown that a reasonably accurate equivalent circuit of a long-wire antenna used with a radio set near a finitely conducting

[12] *G. Baker and W. J. Stark, EMP Vulnerability Analysis of Radio Sets AN/PRC-77, AN/VRC-64, and AN/GRC-160, Harry Diamond Laboratories TR-1747 (April 1976).*

ground plane can be developed from a transmission-line model of the antenna. The accuracy of this model was determined by comparing experimental data with pertinent quantities such as antenna impedance and short-circuit current for various angles of the incident field.

We developed a lumped-parameter-network (LPN) representation of the antenna so that this network could be used in combination with the time-domain short-circuit current at the antenna terminal in a network analysis of the antenna-radio combination. Finally, we have developed a network model of the front end of the radio used with the antenna so that this network could be used as a load for the Thevenin equivalent circuit of the antenna. Computed results for the load circuit when the radio was tuned to various frequencies showed good agreement with experimental data.

The technique used for the analysis of the long-wire antenna with its radio is useful, since it can be generalized to other types of antennas. A frequency-domain solution already exists for many types of antennas and the major problem remaining is to perform an accurate LPN synthesis of the antenna impedances. It may well be that a simple approach such as the one used here is applicable to many types of antennas-- i.e., synthesis of the antenna impedance in terms of a series sum of parallel resonant circuits. The source current or source voltage can be obtained simply from Fourier analysis of the frequency-domain solution.

ACKNOWLEDGEMENT

The authors would like to thank Charles A. Berkley, Jr., for his assistance on this project. Mr. Berkley contributed to the test plan for the experiments and performed all the measurements, taking care to minimize any experimental error. He also transferred the data in digital form to an on-line computer for subsequent data analysis.

LITERATURE CITED

(1) Department of the Army, Operator's and Organizational Maintenance Manual, Including Repair Parts List: Radio Set AN/PRC-77, TM 11-5820-667-12 (June 1967).

(2) P. P. Toulios, Antenna User's Manual for Cylindrical Antennas, Vol I, Illinois Institute of Technology Research Institute (January 1974).

(3) E. D. Sunde, Earth Conduction Effects in Transmission Systems, Dover Publications, Inc., New York (1968).

(4) W. E. Scharfman, K. A. Graf, and E. F. Vance, Analysis of Coupling to Horizontal and Vertical Wires, Stanford Research Institute, SRI Technical Memorandum No. 22 (1972).

(5) E. F. Vance, Defense Nuclear Agency EMP Handbook, 2114, Ch 11, Coupling to Cables (December 1974).

(6) W. J. Stark, Transient Response of a Log-Periodic Antenna Based on Broadband CW Measurements, Harry Diamond Laboratories TR-1792 (April 1977).

(7) E. A. Guillemin, Synthesis of Passive Networks, John Wiley & Sons, Inc., New York (1957).

(8) Janis Klebers, User's Manual for the NLINE Multiconductor Transmission-Line Computer Code, Harry Diamond Laboratories TR-1803 (May 1977).

(9) Eugene L. Patrick and Spencer L. SooHoo, Transportable Electromagnetic Pulse Simulator (TEMPS) Field Mapping Report, Harry Diamond Laboratories TR-1743 (September 1976).

(10) E. C. Jordan and K. G. Balmain, Electromagnetic Waves and Radiating Systems, Prentice-Hall, Inc., Englewood Cliffs, NJ (1968).

(11) Department of the Army, DS, GS and Depot Maintenance Manual: Radio Set AN/PRC-77, TM 11-5820-667-35 (16 February 1968).

(12) G. Baker and W. J. Stark, EMP Vulnerability Analysis of Radio Sets AN/PRC-77, AN/VRC-64, and AN/GRC-160, Harry Diamond Laboratories TR-1747 (April 1976).

APPENDIX A.--COMPUTER-AIDED SYSTEM SIMULATION ERROR

A-1. SOURCES OF ERROR

Considerable controversy surrounds the validity of using computer-simulated electromagnetic pulse (EMP) coupling sources and circuit response to predict circuit damage. The controversy stems from the lack of a comprehensive error analysis for the computer network analysis. This appendix considers the feasibility of such an error analysis and examines the variance in AN/PRC-77 damage predictions due to theoretical verses experimental EMP-induced antenna waveforms.

All simulation programs are subject to errors due primarily to

(a) Incomplete models

(b) Simplified driving function representation

(c) Limited experimental data

(d) Variance in real system component characteristics

(e) Numerical differentiation/integration

(f) Nonlinear equation convergence check tolerances

It has been the express object of the AN/PRC-77 analysis to minimize error-source categories (a) through (c). Sections 3.1, 3.2, and 5.2 in the main report discuss the model verification for the antenna and circuit responses. Verification is based on the "proof of the pudding, seeing is believing" adages. That the code-predicted system response compares favorably with oscilloscope traces indicates an adequately modeled system.

Error-source category (d) affects the circuit modeling for the AN/PRC-77 in that a signal tolerance of ±20 percent is acceptable in the real circuit.[1] An inherent uncertainty in the real system response broadens the admissible range for the modeled circuit's behavior. It should also be noted here that the 20-percent tolerance in voltage propagates as a 40-percent spread in dissipated power, such that a factor of 2.25 separates the low tolerance power from the high tolerance power.

---

[1] *Department of the Army, DS, GS and Depot Maintenance Manual: Radio Set AN/PRC-77, TM 11-5820-667-35 (16 February 1968).*

APPENDIX A

The numerical problems associated with the computer codes themselves (error-source categories (e) and (f)) have been subjected to scrutiny during the code development. The amount of error introduced by numerical techniques is a function of the system under analysis. In general, the more complex the system and the more parameters which come into play to characterize that system, the greater is the associated numerical error. To rigorously quantify the numerical error would be a costly and time-consuming task.

A-2. DAMAGE PREDICTION

Remembering that the ultimate aim of the system analysis is to assess possible circuit damage from EMP-induced transient overstress, the error associated with the damage indicators calculated by the circuit analysis is brought into question. Such a question cannot be fully treated by the study of one system. Obviously, the errors associated with the damage indicators fall into the same six categories listed in section A-1. The two predominating sources of uncertainty for simulating damage are, specifically,

(a) The inherent large spread in experimental power-to-damage semiconductor components (error-source category (d)).

(b) The intractability of device behavior at the instant of failure (error-source category (a)).

The large power-to-damage spread (~1 decade for many semiconductors) is due to the catastrophic nature of the junction failure mechanism. Failure is an irreversible thermal phenomenon. Simulation of the device behavior in the failure region involves the solution of a nonlinear heat-flow equation requiring the determination of parameters (some temperature dependent) relating to the structure and composition of the device in question. To avoid the laborious task of characterizing failure behavior and to avoid the wide dispersion of the device characteristics at thermal breakdown, no attempt is made to simulate failure during the circuit simulation. Instead, the device prefailure characteristic equations are used to simulate device behavior regardless of incident signal strength. During the time-domain circuit-response simulation, the device junction instantaneous power P(t) is recorded. Following the simulation, auxiliary subroutines are called which determine whether a given junction would have experienced enough power to precipitate thermal breakdown. This approach is consistent with the experimental method used to establish device damage thresholds. In that case, square-pulse waveforms incident at the junction terminals are incrementally increased until thermal breakdown is affected. Failure is characterized by a sudden surge of current through the device at some point during the pulse duration (fig. A-1).

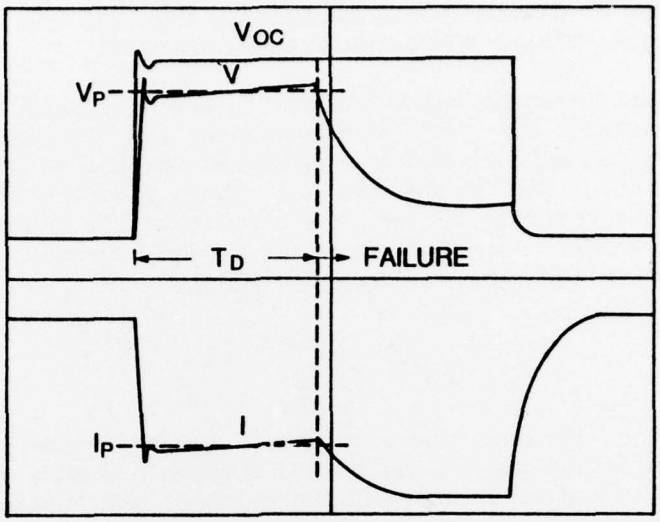

Figure A-1. Typical damage oscillogram.

The pre-failure power ($I_d \cdot V_d$) and pre-failure pulse duration are then used as the damage threshold indicators. Thus, it is unnecessary to track device post-failure behavior since one knows the pre-thermal breakdown device characteristics and the failure threshold.

If we assume that the power to damage a device may be characterized as an experimentally determined function of pulse duration, $P_d = f(t)$, then the damage criteria for an arbitrary power signature, $P(\lambda)$, may be characterized by the following integral equation.[2]

$$\int_0^t P(\lambda) \frac{d}{d(t-\lambda)} \left(\frac{1}{f(t-\lambda)} \right) d\lambda \geq 1 \quad .$$

The above equation follows from the application of Duhamel's theorem to the rate of heat production in the semiconductor material. The equation states that we can expect damage if the result of the integral exceeds unity.

---

[2] *Dante M. Tasca, Joseph E. Peden, and John L. Andrews, Theoretical and Experimental Studies of Semiconductor Device Degradation due to High Power Electrical Transients, G.E. Document No. 73[illegible]289 (December 1973).*

APPENDIX A

A-3. COMPARISON OF DAMAGE THRESHOLD DUHAMEL INTEGRAL FOR EXPERIMENTAL VERSES SIMULATED ANTENNA RESPONSE

The Duhamel integral value for the power dissipated in the 2N3375 can be calculated for both field-measured and LPN-simulated antenna responses using the circuit model constructed for the AN/PRC-77 response to the long wire. The comparison of these values will provide some indication of the sensitivity of the circuit to the approximation used in the antenna model. In performing the Duhamel integral, the familiar Wunsch-Bell damage equation was used for $P_d(t)$,

$$P_d(t) = \frac{K}{t_d^{\frac{1}{2}}}$$

where P is the failure power threshold and t_d is the pulse duration which precipitates failure. Figures A-2 through A-5 show comparisons of the base- emitter and collector-emitter voltages and instantaneous power for the field-measured and LPN-simulated antenna responses.

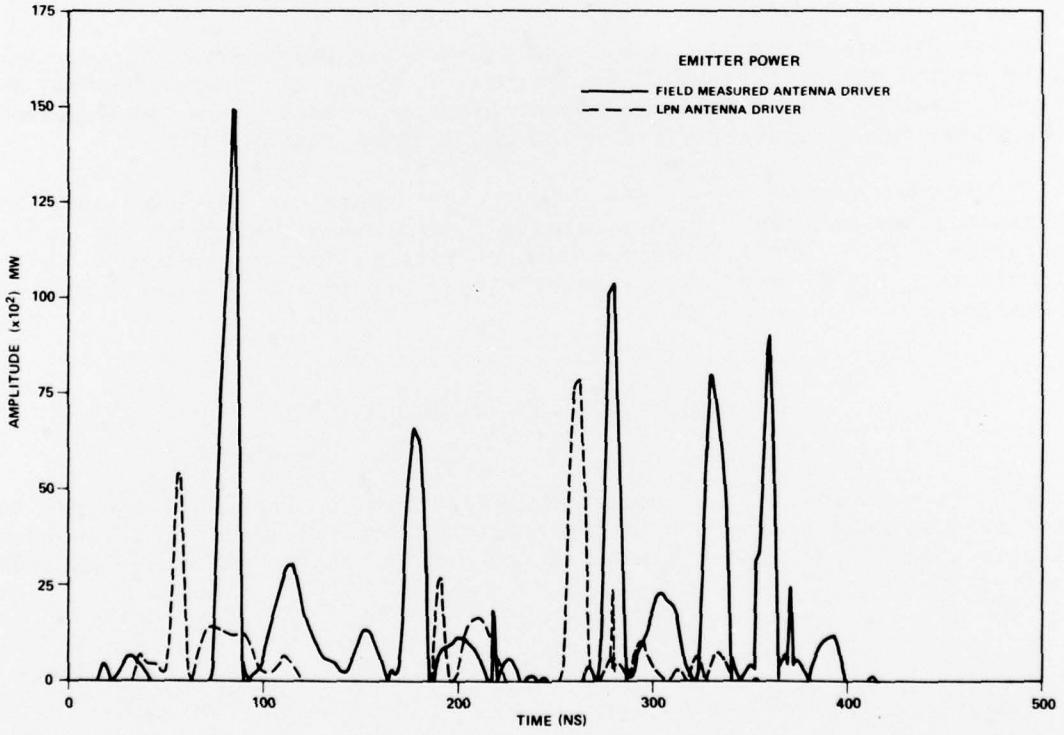

Figure A-2. Emitter power.

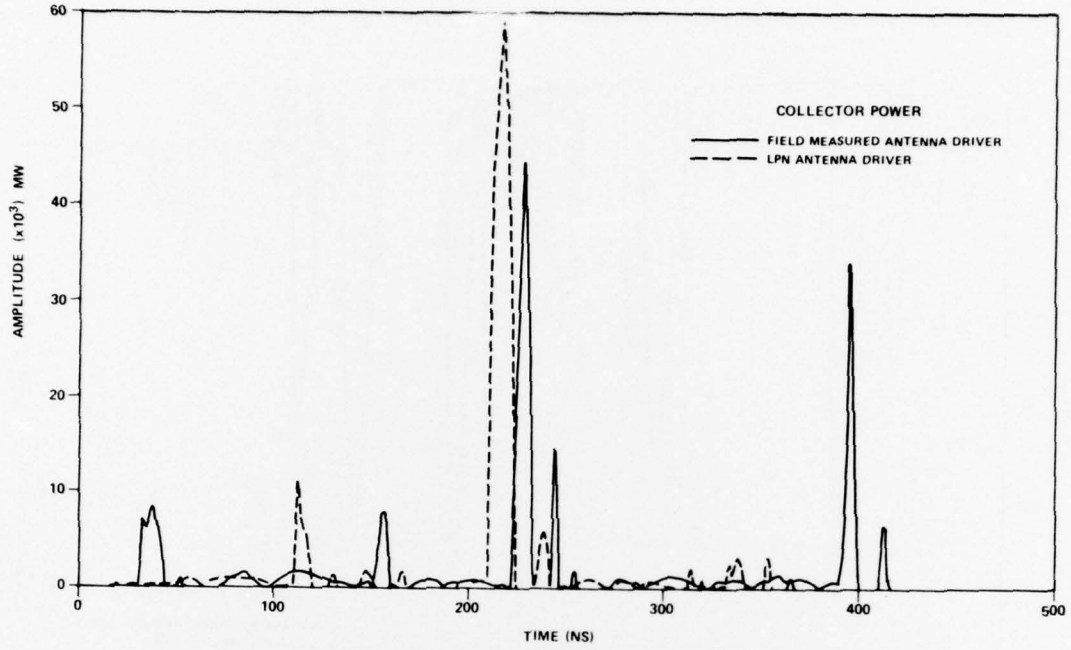

Figure A-3. Collector power.

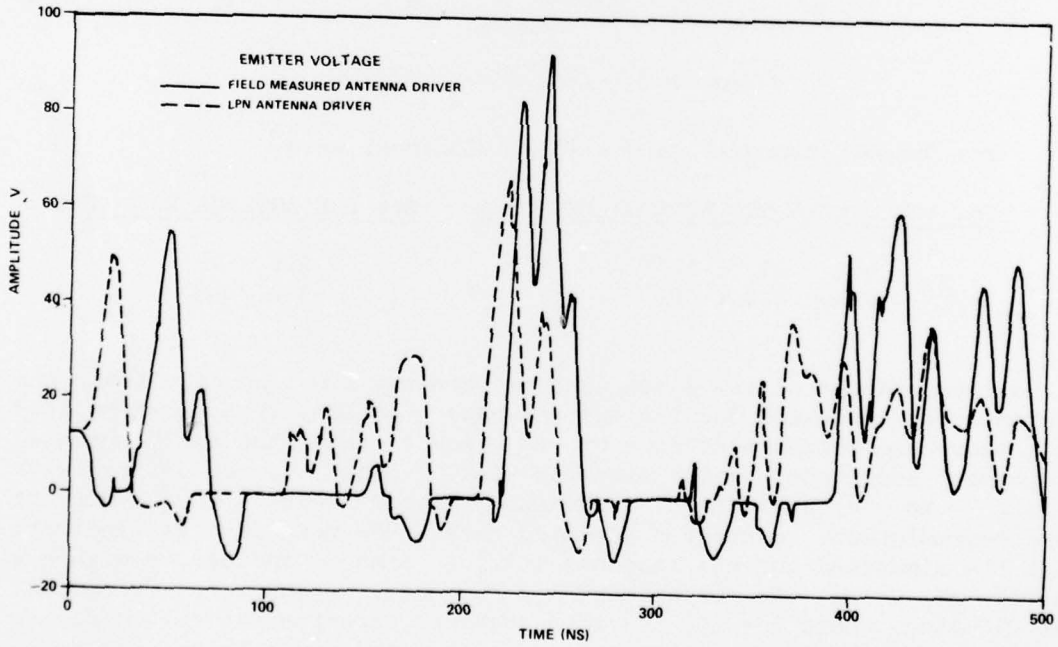

Figure A-4. Emitter voltage.

APPENDIX A

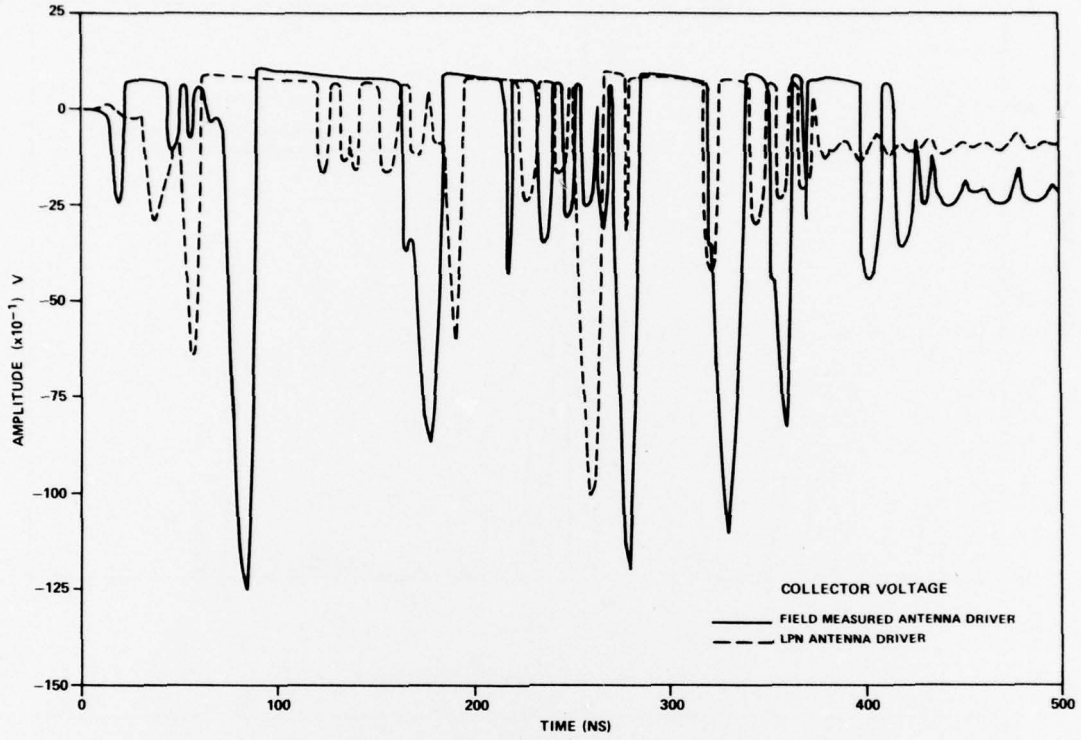

Figure A-5. Collector voltage.

The Duhamel integral values (dimensionless) were

	for FIELD-MEASURED ANTENNA RESPONSE	for LPN ANTENNA RESPONSE
E-B	$13. \times 10^{-4}$	6.5×10^{-4}
C-B	2.5×10^{-3}	3.8×10^{-3}

A maximum factor of two difference between the LPN and field-antenna response is indicated for the emitter-base junction. The LPN-simulated collector-base response differs by 34 percent from the field-measured response. Admittedly, this exercise leaves much to be desired with regard to establishing confidence bands for the circuit damage-prediction techniques employed here. However, it does indicate that the simulated antenna response induces damage indicators within a factor of 2 of the experimental response. For a log normal distribution, where $2 = 10^{1}$ (as in a typical experimental device damage curve), a factor of 2 is well within one standard deviation of the mean. Note again the factor of 2.25 spread of the acceptable signal power limits discussed in section A-1.

A-4. CONCLUSIONS

As evidenced by our discussion, a consideration of the error inherent in system simulation becomes almost philosophical. Given the manifold error sources and complex error interactions, the analyst is forced by time and cost considerations to justify his simulation results solely on visual comparison of computer-generated responses with real data. It is suggested that such justification is adequate for the purposes of EMP vulnerability analysis, given the spread in experimental device failure data. Given the multiplicity of error sources with their complex interplay and propagation, a comprehensive error analysis for most real system-response simulations is not practical. The real merit of a computer system simulation occurs when it is used to produce conservative estimates of system vulnerability levels: adjusting those parameters most subject to error to their worst-case values.

DISTRIBUTION

DEFENSE DOCUMENTATION CENTER
CAMERON STATION, BUILDING 5
ALEXANDRIA, VA 22314
ATTN DDC-TCA (12 COPIES)

COMMANDER
US ARMY MATERIEL DEVELOPMENT
& READINESS COMMAND
5001 EISENHOWER AVENUE
ALEXANDRIA, VA 22333
ATTN DRXAM-TL, HQ TECH LIBRARY
ATTN DRCRP/MG C. M. MCKEEN, JR.
ATTN DRCRP-M/COL R. W. SPECKER
ATTN DRCPM-SCM-WF
ATTN DRCDE-D/MR. HUNT
ATTN DRCDE-D/COL J. F. BLEECKER
ATTN DRCDE, DIR FOR DEV & ENGR
ATTN DRCDE-DE/H. DARRACOTT
ATTN DRCMS-I/DR. R. P. UHLIG
ATTN DRCMS-I/MR. E. O'DONNEL
ATTN DRCDMD-ST/N. L. KLEIN

COMMANDER
US ARMY ARMAMENT MATERIEL
READINESS COMMAND
ROCK ISLAND ARSENAL
ROCK ISLAND, IL 61201
ATTN DRSAR-ASF, FUZE &
MUNITION SPT DIV
ATTN DRSAR-PDM/J. A. BRINKMAN
ATTN DRCPM-VFF

COMMANDER
USA MISSILE & MUNITIONS CENTER
& SCHOOL
REDSTONE ARSENAL, AL 35809
ATTN ATSK-CTD-F

DIRECTOR
US ARMY BALLISTIC RESEARCH LABORATORY
ABERDEEN PROVING GROUND, MD 21005
ATTN DRDAR-TSB-S (STINFO)

DEFENSE ADVANCED RESEARCH
PROJECTS AGENCY
1400 WILSON BLVD
ARLINGTON, VA 22209
ATTN TECH INFORMATION OFFICE
ATTN DIR, STRATEGIC TECHNOLOGY
ATTN DIR, TACTICAL TECHNOLOGY

DIRECTOR
DEFENSE COMMUNICATION ENG CENTER
1860 WIEHLE AVENUE
RESTON, VA 22090
ATTN R104, M. J. RAFFENSPERGER
ATTN R800, R. E. LYONS
ATTN R320, A. IZZO

DIRECTOR
DEFENSE INTELLIGENCE AGENCY
WASHINGTON, DC 20301
ATTN DI-2, WEAPONS & SYSTEMS DIV

DIRECTOR
DEFENSE NUCLEAR AGENCY
WASHINGTON, DC 20305
ATTN PETER HAAS, DEP DIR,
SCIENTIFIC TECHNOLOGY
ATTN RAEV, MAJ S. O. KENNEDY, SR.
ATTN VLIS, LTC ADAMS

DEPARTMENT OF DEFENSE
DIRECTOR OF DEFENSE RESEARCH
& ENGINEERING
WASHINGTON, DC 20301
ATTN DEP DIR (TACTICAL WARFARE PROGRAMS)
ATTN DEP DIR (TEST & EVALUATION)
ATTN DEFENSE SCIENCE BOARD
ATTN ASST DIR SALT SUPPORT GP/MR. J. BLAYLOCK

CHAIRMAN
JOINT CHIEFS OF STAFF
WASHINGTON, DC 20301
ATTN J-3, NUCLEAR WEAPONS BR
ATTN J-3, EXER PLANS & ANALYSIS DIV
ATTN J-5, NUCLEAR DIR NUCLEAR POLICY BR
ATTN J-5, REQUIREMENT & DEV BR
ATTN J-6, COMMUNICATIONS-ELECTRONICS

DEPARTMENT OF DEFENSE
JOINT CHIEFS OF STAFF
STUDIES ANALYSIS & GAMING AGENCY
WASHINGTON, DC 20301
ATTN STRATEGIC FORCES DIV
ATTN GEN PURPOSE FORCES DIV
ATTN TAC NUC BR
ATTN SYS SUPPORT BR

ASSISTANT SECRETARY OF DEFENSE
PROGRAM ANALYSIS AND EVALUATION
WASHINGTON, DC 20301
ATTN DEP ASST SECY (GEN PURPOSE PROG)
ATTN DEP ASST SECY (REGIONAL PROGRAMS)
ATTN DEP ASST SECY (RESOURCE ANALYSIS)

DEPARTMENT OF THE ARMY
OFFICE, SECRETARY OF THE ARMY
WASHINGTON, DC 20301
ATTN ASST SECRETARY OF THE ARMY (I&L)
ATTN DEP FOR MATERIEL ACQUISITION
ATTN ASST SECRETARY OF THE ARMY (R&D)

DEPARTMENT OF THE ARMY
ASSISTANT CHIEF OF STAFF FOR INTELLIGENCE
WASHINGTON, DC 20301
ATTN DAMI-OC/COL J. A. DODDS
ATTN DAMI-TA/COL F. M. GILBERT

DISTRIBUTION (Cont'd)

US ARMY SECURITY AGENCY
ARLINGTON HALL STATION
4000 ARLINGTON BLVD
ARLINGTON, VA 22212
ATTN DEP CH OF STAFF RESEARCH
& DEVELOPMENT

DEPARTMENT OF THE ARMY
US ARMY CONCEPTS ANALYSIS AGENCY
8120 WOODMONT AVENUE
BETHESDA, MD 20014
ATTN COMPUTER SUPPORT DIV
ATTN WAR GAMING DIRECTORATE
ATTN METHODOLOGY AND RESOURCES DIR
ATTN SYS INTEGRATION ANALYSIS DIR
ATTN JOINT AND STRATEGIC FORCES DIR
ATTN FORCE CONCEPTS AND DESIGN DIR
ATTN OPERATIONAL TEST AND EVAL AGENCY

DIRECTOR
NATIONAL SECURITY AGENCY
FORT GEORGE G. MEADE, MD 20755

COMMANDER-IN-CHIEF
EUROPEAN COMMAND
APO NEW YORK, NY 09128

HEADQUARTERS
US EUROPEAN COMMAND
APO NEW YORK, NY 09055

DIRECTOR
WEAPONS SYSTEMS EVALUATION GROUP
OFFICE, SECRETARY OF DEFENSE
400 ARMY-NAVY DRIVE
WASHINGTON, DC 20305
ATTN DIR, LT GEN GLENN A. KENT

DEPARTMENT OF THE ARMY
DEPUTY CHIEF OF STAFF FOR
OPERATIONS & PLANS
WASHINGTON, DC 20301
ATTN DAMO-RQD/COL E. W. SHARP
ATTN DAMO-SSP/COL D. K. LYON
ATTN DAMO-SSN/LTC R. E. LEARD
ATTN DAMO-SSN/LTC B. C. ROBINSON
ATTN DAMO-RQZ/COL G. A. POLLIN, JR.
ATTN DAMO-TCZ/MG T. M. RIENZI
ATTN DAMO-ZD/A. GOLUB
ATTN DAMO-RQA/COL M. T. SPEIR

DEPARTMENT OF THE ARMY
CHIEF OF RESEARCH, DEVELOPMENT
AND ACQUISITION OFFICE
WASHINGTON, DC 20301
ATTN DAMA-RAZ-A/R. J. TRAINOR
ATTN DAMA-CSM-N/LTC OGDEN
ATTN DAMA-WSA/COL W. E. CROUCH, JR.
ATTN DAMA-WSW/COL L. R. BAUMANN
ATTN DAMA-CSC/COL H. C. JELINEK

CHIEF OF RESEARCH, DEVELOPMENT
AND ACQUISITION OFFICE (Cont'd)
ATTN DAMA-CSM/COL H. R. BAILEY
ATTN DAMA-WSZ-A/MG D. R. KEITH
ATTN DAMA-WSM/COL J. B. OBLINGER, JR.
ATTN DAMA-PPR/COL D. E. KENNEY

COMMANDER
BALLISTIC MISSILE DEFENSE SYSTEMS
P.O. BOX 1500
HUNTSVILLE, AL 35807
ATTN BMDSC-TEN/MR. JOHN VEFNEMAN

COMMANDER
US ARMY FOREIGN SCIENCE
AND TECHNOLOGY CENTER
220 SEVENTH ST., NE
CHARLOTTESVILLE, VA 22901

DIRECTOR
US ARMY MATERIEL SYSTEMS ANALYSES ACTIVITY
ABERDEEN PROVING GROUND, MD 21005
ATTN DRXSY-C/DON R. BARTHEL
ATTN DRXSY-T/P. REID

COMMANDER
US ARMY SATELLITE COMMUNICATIONS AGENCY
FT. MONMOUTH, NJ 07703
ATTN LTC HOSMER

DIRECTOR
BALLISTIC RESEARCH LABORATORIES
ABERDEEN PROVING GROUND, MD 21005
ATTN DRXBR-XA/MR. J. MESZAROS

COMMANDER
US ARMY AVIATION SYSTEMS COMMAND
12TH AND SPRUCE STREETS
ST. LOUIS, MO 63160
ATTN DRCPM-AAH/ROBERT HUBBARD

DIRECTOR
EUSTIS DIRECTORATE
US ARMY AIR MOBILITY R&D LABORATORY
FORT EUSTIS, VA 23604
ATTN SAVDL-EU-MOS/MR. S. POCILUYKO
ATTN SAVDL-EU-TAS(TETRACORE)

COMMANDER
2D BDE, 101ST ABN DIV (AASLT)
FORT CAMPBELL, KY 42223
ATTN AFZB-KB-SO
ATTN DIV SIGNAL OFFICER,
AFBZ-SO/MAJ MASON

COMMANDER
US ARMY COMMUNICATIONS RES & DEV COMMAND
FT. MONMOUTH, NJ 07703
ATTN PM, ATACS/DRCPM-ATC/LTC DOBBINS
ATTN DRCPM-ATC-TM

US ARMY COMMUNICATIONS RES & DEV
COMMAND (Cont'd)
ATTN PM, ARTADS/DRCPM-TDS/BG A. CRAWFORD
ATTN DRCPM-TDS-TF/COL D. EMERSON
ATTN DRCPM-TDS-TO
ATTN DRCPM-TDS-FB/LTC A. KIRKPATRICK
ATTN PM, MALOR/DRCPM-MALR/COL W. HARRISON
ATTN PM, NAVCOM/DRCPM-NC/
COL C. MCDOWELL, JR.
ATTN PM, REMBASS/DRCPM-RBS/
COL R. COTTEY, SR.
ATTN DRSEL-TL-IR/MR. R. FREIBERG
ATTN DRSEL-SA/NORMAN MILLSTEIN
ATTN DRSEL-MA-C/J. REAVIS
ATTN DRSEL-CE-ES/J. A. ALLEN

COMMANDER
US ARMY MISSILE MATERIEL
READINESS COMMAND
REDSTONE ARSENAL, AL 35809
ATTN DRSMI-FRR/DR. F. GIPSON
ATTN DRCPM-HA/COL P. RODDY
ATTN DRCPM-LCCX/L. B. SEGGEL (LANCE)
ATTN DRCPM-MD/GENE ASHLEY (PATRIOT)
ATTN DRCPM-MP
ATTN DRCPM-PE/COL SKEMP (PERSHING)
ATTN DRCPM-SHO
ATTN DRCPM-TO
ATTN DRSMI-R, RDE & MSL DIRECTORATE

COMMANDER
US ARMY ARMAMENT RESEARCH
& DEVELOPMENT COMMAND
DOVER, NJ 07801
ATTN DRDAR-ND-V/DANIEL WAXLER

COMMANDER
US ARMY TANK/AUTOMOTIVE MATERIEL
READINESS COMMAND
WARREN, MI 48090
ATTN DRSI-RHT/MR. P. HASEK
ATTN DRCPM(XM-L)/MR. L. WOOLCOT
ATTN DRCPM-GCM-SW/MR. R. SLAUGHTER

PRESIDENT
DA, HA, US ARMY ARMOR AND
ENGINEER BOARD
FORT KNOX, KY 40121
ATTN STEBB-MO/MAJ SANZOTERRA

COMMANDER
WHITE SANDS MISSILE RANGE
WHITE SANDS MISSILE RANGE, NM 88002
ATTN STEWS-TE-NT/MARVIN SQUIRES

COMMANDER
TRASANA
SYSTEM ANALYSIS ACTIVITY
WHITE SANDS, NM 88002
ATTN ATAA-TDO/DR. D. COLLIER

COMMANDER
197TH INFANTRY BRIGADE
FORT BENNING, GA 31905
ATTN COL WASIAK

COMMANDER
US ARMY COMMUNICATIONS COMMAND
FORT HUACHUCA, AZ 85613
ATTN ACC-AD-C/H. LASITTER (EMP STUDY GP)

COMMANDER
USA COMBINED ARMS COMBAT DEVELOPMENTS
ACTIVITY
FT. LEAVENWORTH, KS 66027
ATTN ATCAC
ATTN ATCACO-SD/LTC L. PACHA
ATTN ATCA/COC/COL HUBBERT
ATTN ATCA-CCM-F/LTC BECKER
ATTN ATSW-TD-3 NUCLEAR STUDY TEAM/
LT D. WILKINS

PROJECT MANAGER
MOBILE ELECTRIC POWER
7500 BACKLICK ROAD
SPRINGFIELD, VA 22150
ATTN DRCPM-MEP

DEPUTY COMMANDER
US ARMY NUCLEAR AGENCY
7500 BACKLICK RD
BUILDING 2073
SPRINGFIELD, VA 22150
ATTN MONA-WE/COL A. DEVERILL

COMMANDER
US ARMY SIGNAL SCHOOL
FT. GORDON, GA 30905
ATTN AISO-CID/BILL MANNELL
ATTN ATST-CTD-CS/CAPT G. ALEXANDER (INTACS)
ATTN ATSO-CID-CS/MR. TAYLOR
ATTN ATSN-CD-OR/MAJ CARR

DIRECTOR
JOINT TACTICAL COMMUNICATIONS OFFICE
FT. MONMOUTH, NJ 07703
ATTN TRI-TAC/NORM BECHTOLD

COMMANDER
US ARMY COMMAND AND GENERAL STAFF COLLEGE
FORT LEAVENWORTH, KS 66027

COMMANDER
US ARMY COMBAT DEVELOPMENTS EXPERIMENTATION
COMMAND
FORT ORD, CA 93941

COMMANDER
HQ MASSTER
FORT HOOD, TX 76544

DISTRIBUTION (Cont'd)

COMMANDER
US ARMY AIR DEFENSE SCHOOL
FORT BLISS, TX 79916
ATTN ATSA-CD

COMMANDER
US ARMY ARMOR SCHOOL
FORT KNOX, KY 40121
ATTN ATSB-CTD (2 COPIES)

COMMANDER
US ARMY AVIATION CENTER
FORT RUCKER, AL 36360
ATTN ATST-D-MS (2 COPIES)

COMMANDER
US ARMY ORDNANCE CENTER AND SCHOOL
ABERDEEN PROVING GROUND, MD 21005
ATTN USAOC&S
ATTN ATSL-CTD

COMMANDER
US ARMY SIGNAL SCHOOL
FORT GORDON, GA 30905
ATTN ATSS-CTD (2 COPIES)

COMMANDER
US ARMY ENGINEER SCHOOL
FORT BELVOIR, VA 22060
ATTN ATSE-CTD (2 COPIES)

COMMANDER
US ARMY INFANTRY SCHOOL
FORT BENNING, GA 31905
ATTN ATSH-CTD (2 COPIES)

COMMANDER
US ARMY INTELLIGENCE CENTER AND SCHOOL
FORT HUACHUCA, AZ 85613
ATTN ATSI-CTD (2 COPIES)

COMMANDER
US ARMY FIELD ARTILLERY SCHOOL
FORT SILL, OK 73503
ATTN ATSF-CTD (2 COPIES)

CHIEF OF NAVAL OPERATIONS
NAVY DEPARTMENT
WASHINGTON, DC 20350
ATTN NOP-932, SYS EFFECTIVENESS DIV
CAPT E. V. LANEY
ATTN NOP-9860, COMMUNICATIONS BR
COR L. LAYMAN
ATTN NOP-351, SURFACE WEAPONS BR
CAPT G. A. MITCHELL
ATTN NOP-622C, ASST FOR NUCLEAR
VULNERABILITY, R. PIACESI

COMMANDER
NAVAL ELECTRONICS SYSTEMS COMMAND, HQ
2511 JEFFERSON DAVIS HIGHWAY
ARLINGTON, VA 20360
ATTN PME-117-21, SANGUINE DIV

HEADQUARTERS, NAVAL MATERIEL COMMAND
STRATEGIC SYSTEMS PROJECTS OFFICE
1931 JEFFERSON DAVIS HIGHWAY
ARLINGTON, VA 20390
ATTN NSP2201, LAUNCHING & HANDLING
BRANCH, BR ENGINEER, P. R. FAUROT
ATTN NSP-230, FIRE CONTROL & GUIDANCE
BRANCH, BR ENGINEER, D. GOLD
ATTN NSP-2701, MISSILE BRANCH,
BR ENGINEER, J. W. PITSENBERGER

COMMANDER
NAVAL SURFACE WEAPONS CENTER
WHITE OAK, MD 20910
ATTN CODE 222, ELECTRONICS & ELECTRO-
MAGNETICS DIV
ATTN CODE 431, ADVANCED ENGR DIV

US AIR FORCE, HEADQUARTERS
DCS, RESEARCH & DEVELOPMENT
WASHINGTON, DC 20330
ATTN DIR OF OPERATIONAL REQUIREMENTS
AND DEVELOPMENT PLANS, S/V &
LTC P. T. DUESBERRY

COMMANDER
AF WEAPONS LABORATORY, AFSC
KIRTLAND AFB, NM 87117
ATTN ES, ELECTRONICS DIVISION
ATTN EL, J. DARRAH
ATTN TECHNICAL LIBARY
ATTN D. I. LAWRY

COMMANDER
AERONAUTICAL SYSTEMS DIVISION, AFSC
WRIGHT-PATTERSON AFB, OH 45433
ATTN ASD/YH, DEPUTY FOR B-1

COMMANDER
HQ SPACE AND MISSILE SYSTEMS ORGANIZATION
P.O. 96960 WORLDWAYS POSTAL CENTER
LOS ANGELES, CA 90009
ATTN S7H, DEFENSE SYSTEMS APL SPO
ATTN XRT, STRATEGIC SYSTEMS DIV
ATTN YAS, SURVIVABILITY OFC

SPACE AND MISSILE SYSTEMS ORGANIZATION
NORTON AFB, CA 92409
ATTN MMH, HARD ROCK SILO DEVELOPMENT

DISTRIBUTION (Cont'd)

COMMANDER
AF SPECIAL WEAPONS CENTER, AFSC
KIRTLAND AFB, NM 87117

ASSISTANT CHIEF OF STAFF
FOR COMMUNICATIONS ELECTRONICS
XVIII AIRBORNE CORPS
FORT BRAGG, NC 28307
ATTN AFZA-CE/LTC K. KILLINGSTEAD

HARRY DIAMOND LABORATORIES
ATTN COMMANDER/
FLYER, I.N./LANDIS, P.E./
SOMMER, H./OSWALD, R. B.
ATTN CARTER, W.W., DR., TECHNICAL
DIRECTOR
ATTN WISEMAN, ROBERT S., DR., DRDEL-CT
ATTN MARCUS, S. M., 003
ATTN KIMMEL, S., PAO
ATTN CHIEF, 0021
ATTN CHIEF, 0022
ATTN CHIEF, LAB 100
ATTN CHIEF, LAB 200
ATTN CHIEF, LAB 300
ATTN CHIEF, LAB 400
ATTN CHIEF, LAB 500
ATTN CHIEF, LAB 600
ATTN CHIEF, DIV 700
ATTN CHIEF, DIV 800
ATTN CHIEF, LAB 900
ATTN CHIEF, LAB 1000
ATTN RECORD COPY, BR 041
ATTN HDL LIBRARY (5 COPIES)
ATTN CHAIRMAN, EDITORIAL COMMITTEE
ATTN CHIEF, 047
ATTN TECH REPORTS, 013
ATTN PATENT LAW BRANCH, 071
ATTN GIDEP OFFICE, 741
ATTN LANHAM, C., 0021
ATTN CHIEF, 0024
ATTN CHIEF, 1010
ATTN CHIEF, 1020 (20 COPIES)
ATTN CHIEF, 1030
ATTN CHIEF, 1040
ATTN CHIEF, 1050

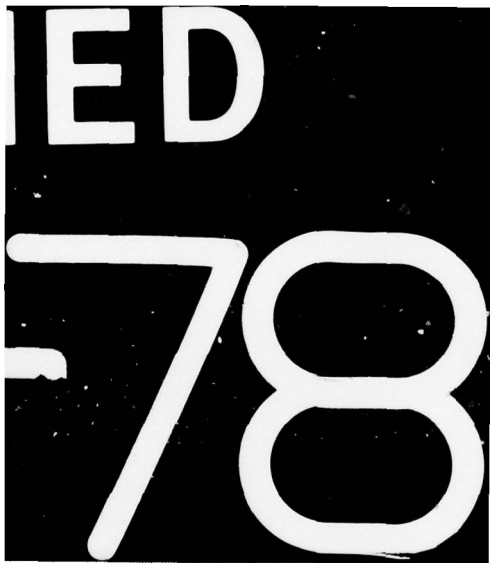
ED
78